Optimization and characterization of a highly-efficient diffraction nanograting for MHz XUV pulses

Ying-Ying Yang,[1,2,3] Frederik Süßmann,[1,4] Sergey Zherebtsov,[1] Ioachim Pupeza,[1,4] Jan Kaster,[1,4] Dennis Lehr,[5] Hans-Jörg Fuchs,[5] Ernst-Bernhard Kley,[5] Ernst Fill,[1,4] Xuan-Ming Duan,[2] Zhen-Sheng Zhao,[2] Ferenc Krausz,[1,4] Sarah L. Stebbings,[1] and Matthias F. Kling[1,*]

[1]*Max-Planck-Institut für Quantenoptik, Hans-Kopfermann-Straße 1, 85748 Garching, Germany*
[2]*Technical Institute of Physics and Chemistry, Chinese Academy of Sciences, 100190 Beijing, China*
[3]*Graduate School of the Chinese Academy of Sciences, 100190 Beijing, China*
[4]*Ludwig-Maximilians-Universität München, Am Coulombwall 1, 85748 Garching, Germany*
[5]*Friedrich-Schiller-Universität Jena, 07737 Jena, Germany*
**matthias.kling@mpq.mpg.de*

Abstract: We designed, fabricated and characterized a nano-periodical highly-efficient blazed grating for extreme-ultraviolet (XUV) radiation. The grating was optimized by the rigorous coupled-wave analysis method (RCWA) and milled into the top layer of a highly-reflective mirror for IR light. The XUV diffraction efficiency was determined to be around 20% in the range from 35.5 to 79.2 nm. The effects of the nanograting on the reflectivity of the IR light and non-linear effects introduced by the nanograting have been measured and are discussed.

OCIS codes: (050.1950) Diffraction gratings; (340.7480) X-rays, soft x-rays, extreme ultraviolet.

References and links

1. P. B. Corkum, "Plasma perspective on strong field multiphoton ionization," Phys. Rev. Lett. **71**(13), 1994–1997 (1993).
2. C. Spielmann, N. H. Burnett, S. Sartania, R. Koppitsch, M. Schnürer, C. Kan, M. Lenzner, P. Wobrauschek, and F. Krausz, "Generation of Coherent X-rays in the Water Window Using 5-Femtosecond Laser Pulses," Science **278**(5338), 661–664 (1997).
3. M. I. Stockman, M. F. Kling, U. Kleineberg, and F. Krausz, "Attosecond nanoplasmonic-field microscope," Nat. Photonics **1**(9), 539–544 (2007).
4. C. Gohle, T. Udem, M. Herrmann, J. Rauschenberger, R. Holzwarth, H. A. Schuessler, F. Krausz, and T. W. Hänsch, "A frequency comb in the extreme ultraviolet," Nature **436**(7048), 234–237 (2005).
5. R. J. Jones, K. D. Moll, M. J. Thorpe, and J. Ye, "Phase-coherent frequency combs in the vacuum ultraviolet via high-harmonic generation inside a femtosecond enhancement cavity," Phys. Rev. Lett. **94**(19), 193201 (2005).
6. A. Ozawa, J. Rauschenberger, Ch. Gohle, M. Herrmann, D. R. Walker, V. Pervak, A. Fernandez, R. Graf, A. Apolonski, R. Holzwarth, F. Krausz, T. W. Hänsch, and T. Udem, "High harmonic frequency combs for high resolution spectroscopy," Phys. Rev. Lett. **100**(25), 253901 (2008).
7. D. C. Yost, T. R. Schibli, and J. Ye, "Efficient output coupling of intracavity high-harmonic generation," Opt. Lett. **33**(10), 1099–1101 (2008).
8. I. Pupeza, T. Eidam, J. Rauschenberger, B. Bernhardt, A. Ozawa, E. Fill, A. Apolonski, T. Udem, J. Limpert, Z. A. Alahmed, A. M. Azzeer, A. Tünnermann, T. W. Hänsch, and F. Krausz, "Power scaling of a high-repetition-rate enhancement cavity," Opt. Lett. **35**(12), 2052–2054 (2010).
9. K. D. Moll, R. J. Jones, and J. Ye, "Output coupling methods for cavity-based high-harmonic generation," Opt. Express **14**(18), 8189–8197 (2006).
10. J. Wu, and H. Zeng, "Cavity-enhanced noncollinear high-harmonic generation for extreme ultraviolet frequency combs," Opt. Lett. **32**(22), 3315–3317 (2007).
11. A. Cingöz, D. Yost, J. Ye, A. Ruehl, M. Fermann, and I. Hartl, "Power Scaling of High-Repetition-Rate HHG," International Conference on Ultrafast Phenomena (2010).
12. M. G. Moharam, and T. K. Gaylord, "Rigorous coupled-wave analysis of metallic surface-relief gratings," J. Opt. Soc. Am. A **3**(11), 1780–1787 (1986).

#139920 - $15.00 USD Received 20 Dec 2010; revised 13 Jan 2011; accepted 13 Jan 2011; published 18 Jan 2011

13. M. G. Moharam, E. B. Grann, D. A. Pommet, and T. K. Gaylord, "Formulation for stable and efficient implementation of the rigorous coupled-wave analysis of binary gratings," J. Opt. Soc. Am. A **12**(5), 1068–1076 (1995).
14. M. G. Moharam, D. A. Pommet, E. B. Grann, and T. K. Gaylord, "Stable implementation of the rigorous coupled-wave analysis for surface-relief gratings: enhanced transmittance matrix approach," J. Opt. Soc. Am. A **12**(5), 1077–1086 (1995).
15. E. D. Palik, G. Ghosh, and E. J. Prucha, eds., *Handbook of Optical Constants of Solids*, (Academic Press New York, 1985).
16. M. Schultze, E. Goulielmakis, M. Uiberacker, M. Hofstetter, J. Kim, D. Kim, F. Krausz, and U. Kleineberg, "Powerful 170-attosecond XUV pulses generated with few-cycle laser pulses and broadband multilayer optics," N. J. Phys. **9**(7), 243 (2007).
17. T. Eidam, F. Röser, O. Schmidt, J. Limpert, and A. Tünnermann, "57 W, 27 fs pulses from a fiber laser system using nonlinear compression," Appl. Phys. B **92**(1), 9–12 (2008).
18. T. Hanke, G. Krauss, D. Träutlein, B. Wild, R. Bratschitsch, and A. Leitenstorfer, "Efficient nonlinear light emission of single gold optical antennas driven by few-cycle near-infrared pulses," Phys. Rev. Lett. **103**(25), 257404 (2009).
19. I. Pupeza, X. Gu, E. Fill, T. Eidam, J. Limpert, A. Tünnermann, F. Krausz, and T. Udem, "Highly sensitive dispersion measurement of a high-power passive optical resonator using spatial-spectral interferometry," Opt. Express **18**(25), 26184–26195 (2010).
20. J. Kaster, I. Pupeza, T. Eidam, C. Jocher, E. Fill, J. Limpert, R. Holzwarth, B. Bernhardt, T. Udem, T. W. Hänsch, A. Tünnermann, and F. Krausz, "Towards MW Average Powers in Ultrafast High-Repetition-Rate Enhancement Cavities," HILAS 2011, Istanbul.

1. Introduction

A well-established technique for the production of attosecond XUV light pulses is high harmonic generation (HHG) in noble gases [1]. In order to utilize the HHG process for frequency conversion from the infrared to the XUV wavelength region, a sufficiently high peak intensity has to be obtained. In conventional HHG experiments amplifiers that boost the pulse energy by sacrificing repetition rate have been widely used [2]. Due to the low repetition rate, such XUV sources have a limited range of applications. In particular for experiments, where a combination of a high XUV flux with low energy/pulse is needed in order to e.g. avoid space charge effects, high repetition rate XUV sources are desired. A prominent example is photoelectron emission microscopy (PEEM), which could be used for exploring ultrafast dynamics in nanostructured surface systems with time resolutions down to the attosecond regime [3]. The realization of MHz XUV sources is, however, a challenging task since high driving pulse energies and peak intensities at these repetition rates are needed for the highly-nonlinear HHG process.

The method of cavity-assisted HHG overcomes these limitations. Here, broadband femtosecond pulses from a mode-locked MHz oscillator are coupled into an external resonant cavity [4–8], in which peak intensities are reached, sufficient to drive intra-cavity HHG at the full repetition rate of the oscillator.

So far, one of the major challenges in cavity-assisted HHG is to efficiently extract the generated high harmonics from the enhancement cavity without influencing the cavity performance. Because intra-cavity generated XUV radiation propagates along the direction of the fundamental beam, it will be blocked and absorbed by the cavity mirrors, which are only highly-reflective for the propagating fundamental light. Thus, an optical element allowing for the output coupling of the intra-cavity generated XUV light is needed, which has high efficiency while exhibiting minimal losses for the fundamental light and also in any other way does not influence the cavity performance.

Several XUV output couplers have been proposed. The first enhancement cavity based HHG systems employed a thin intra-cavity sapphire plate at Brewster's angle for the infrared, while reflecting the XUV radiation [4–6] away from the fundamental radiation beam path. This method nevertheless introduces significant group-velocity dispersion and nonlinear phase shifts at high intensities. To overcome this problem, other methods were proposed, using a small hole in the curved mirror after the intra-cavity focus, where the XUV is generated, or employing a slotted mirror and two colliding pulses to produce non-collinear HHG [9,10].

#139920 - $15.00 USD Received 20 Dec 2010; revised 13 Jan 2011; accepted 13 Jan 2011; published 18 Jan 2011

However, these methods suffer from increasing additional intra-cavity diffraction losses for the fundamental light and a complex implementation, respectively.

As an alternative to the above mentioned methods, Yost and associates [7] reported a small-period relief diffraction grating for XUV light as an output coupler, which is etched directly into the surface of one of the dielectric mirrors of the cavity. This method overcame the major difficulties by adding minimal intra-cavity loss, and by permitting large buildup peak intensities without introducing nonlinear phase shifts to the cavity resonance. To this day, among the intra-cavity generated XUV output coupling techniques this method is the most promising one from the point of view of power scalability [11]. The maximum theoretical output coupling efficiency at a wavelength of 65 nm, for which the grating design was optimized, amounted to roughly 10%.

In this paper, we report on the design, fabrication and characterization of a nano-period grating, which, in contrast to the one presented in [7] is blazed in order to increase the diffraction and thus output coupling efficiency. The blazed grating was designed such that it serves as a diffractive element for the XUV and acts as high-reflective mirror for the fundamental light. We have theoretically studied and optimized the design of such a nano-periodical grating to increase the XUV diffraction efficiency to above 20%. Moreover, we characterized the grating using a XUV light source within the wavelength range of 35.5-79.2 nm and verified its high diffraction efficiency in our experiment. In addition, the influence of the grating structure on the reflectivity of the fundamental IR wavelength and nonlinear effects owed to the nanograting were measured.

2. Optimization of the grating

We first compare theoretically two diffraction grating designs (see Fig. 1), one of which is a relief grating based on the one used by Yost *et al.* [7], the other one is a blazed nanograting, which can lead to higher diffraction efficiency. To determine the optimum design parameters and evaluate the diffraction efficiencies of both gratings, we apply a rigorous coupled-wave analysis method (RCWA) [12–14]. It allows for an arbitrary complex permittivity to be used for the material and thus avoids the infinite conductivity approximation. The wavelength dependent dielectric constants used in these calculations are based on experimental data [15].

The goal of our optimization was to obtain high coupling efficiency between 35.5 and 79.2 nm, corresponding to the 13th to 29th harmonics of a fundamental wavelength of 1030 nm. One motivation for the optimization of the efficiency in this wavelength range comes from the possibility to conduct high resolution spectroscopy of the 1s-2s transition in He^+ at around 61 nm with extreme precision [4,6]. It should be stressed that the choice of the IR wavelength range for the design can be easily varied.

The nano-period grating structure is implemented on a multi-layer dielectric mirror, which is designed as a near-perfect reflector for the fundamental wavelength of 1030 nm with s-polarization. The grating is structured into the uppermost SiO_2 layer of the multi-layer mirror.

The optimization parameters include the incidence angle, groove period, groove depth, the duty cycle, and blaze angle. In Fig. 1c we compare the optimized diffraction efficiencies in the −1st order (higher orders are less efficient) within the given wavelength range for a relief and a blazed nanograting. Note that the fundamental light is only present in the 0th order of diffraction, such that for a structure with optimized −1st diffraction order for the XUV, these two wavelength ranges can be easily separated.

#139920 - $15.00 USD Received 20 Dec 2010; revised 13 Jan 2011; accepted 13 Jan 2011; published 18 Jan 2011

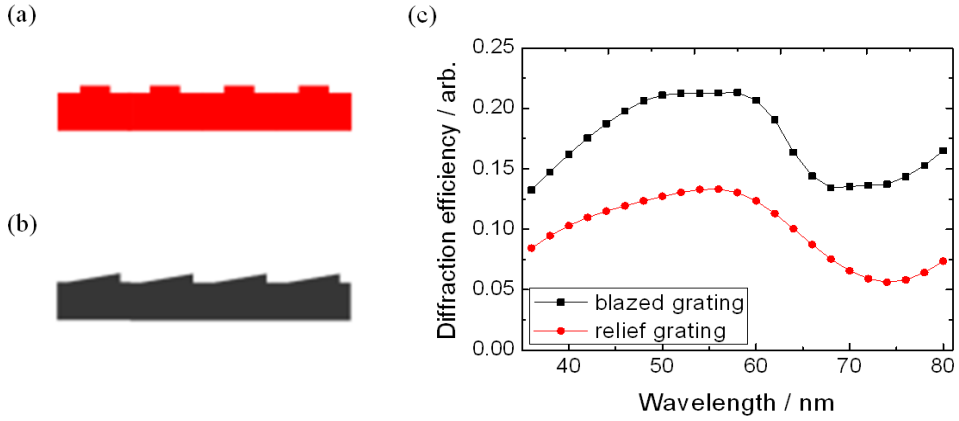

Fig. 1. Comparison of the diffraction efficiency of a relief nanograting (a) and a blazed nanograting (b). Theoretically, the blazed grating can achieve an efficiency of around 20%, which is considerably higher than for a relief grating (around 10%), (c).

The parameters for an optimized relief grating (incidence angle: 70 degrees, grove period: 420 nm, groove depth: 40 nm, duty cycle: 40%) based on the RCWA method exhibit only small differences to the nanograting used by Yost *et al*. giving a diffraction efficiency of about 10% over the studied wavelength range. For the blazed grating the optimized parameters were identified for an incidence angle of 72 degrees, 510 nm groove period, 46 nm groove depth, 70% duty cycle, and a blaze angle of 3.6 degrees. The results of the theoretical simulations for this blazed grating are compared to the relief grating in Fig. 1c. The blazed grating could achieve an efficiency of up to about 20%, which is considerably higher than for the relief grating with approx. 10%. Between the 17th and 21st harmonics (50 nm to 60 nm), the blazed nanograting is found to provide a diffraction efficiency in the −1st order even exceeding 20%.

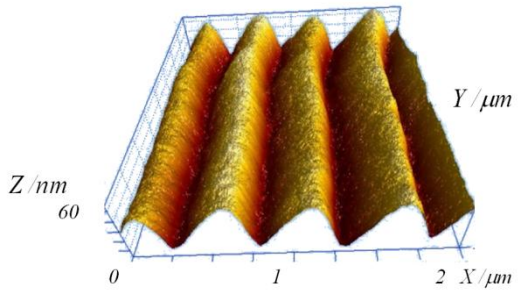

Fig. 2. AFM image of the nanostructured blazed grating. The grating is etched into the uppermost SiO_2 layer. The groove period is 510 nm; groove depth is 60nm and aspect ratio is 70%.

To fabricate the grating, we used the dielectric mirror as the substrate, which is an IR near-perfect reflector (Layertec), R > 99.95% at 1000-1040 nm. Firstly, the substrate was coated with the electron beam resist ARP 617.03. The blazed resist profile was created with the electron beam lithography system Vistec SB350 using a variable dose approach. After the development of the resist mask, it was proportionally transferred into the substrate by ICP-RIE (inductive coupled plasma-reactive ion etching). We employed CHF_3 as process gas and O2-ICP-RIE to remove all organic residues after this transfer. On account of limitations in the manufacturing process, the blazed grating structure had a groove depth of 60 nm. Figure 2 depicts an atomic force microscopy (AFM) image of the produced blazed nanograting.

#139920 - $15.00 USD Received 20 Dec 2010; revised 13 Jan 2011; accepted 13 Jan 2011; published 18 Jan 2011

3. XUV diffraction efficiency measurements

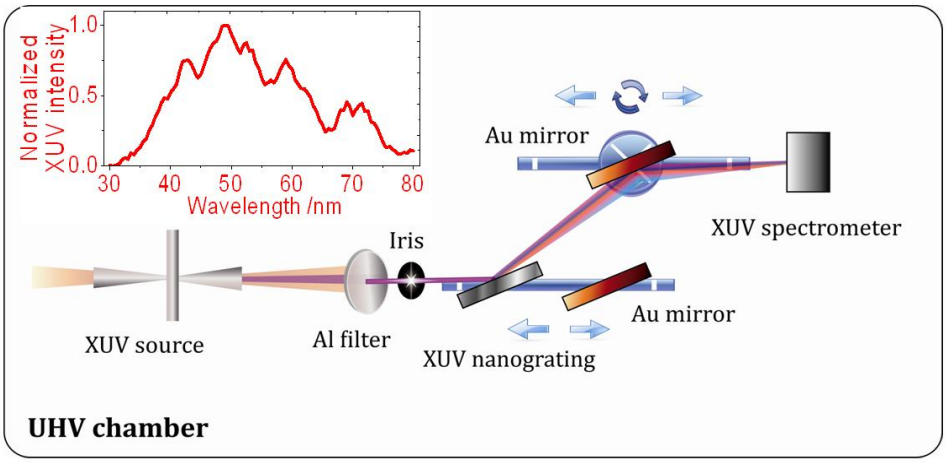

Fig. 3. Illustration of the experimental setup for the diffraction efficiency measurements. The entire setup is placed in a vacuum chamber. The broadband XUV radiation (see inset) is generated by a few-cycle phase-stabilized Ti:Sa laser pulse (750 nm, 4 fs) via HHG in a Xe gas jet. An aluminium filter allows transmission of XUV light below 79.2 nm while removing the residual IR light. The XUV is either diffracted by the blazed nanograting or reflected by a flat gold mirror and then steered into an XUV spectrometer by another gold mirror. In order to compensate for the angular dispersion of the nanograting the second gold mirror could be translated and rotated.

To experimentally characterize the performance of the blazed nanograting, the setup sketched in Fig. 3 was used. Briefly, few-cycle IR laser pulses (750 nm, 4 fs) were used to generate a broadband XUV spectrum by HHG [16] within a Xe gas jet at peak intensities exceeding 10^{13} W/cm^2 in the focus. The gas target is contained within a nickel tube with an inner diameter of 3 mm. Both XUV and IR laser pulses propagate collinearly after the gas target. A 200 nm thick Al filter is used to remove the fundamental laser beam and low order harmonics. An iris with a diameter of 3 mm was placed after the Al filter to ensure that only the nanograting (measuring 4 x 10 mm) etched into the top of the dielectric mirror was illuminated by the XUV beam (rather than the surface of dielectric mirror). After either diffraction from the nanograting or reflection from a flat gold mirror, the XUV light is imaged into a scanning XUV monochromator for the setup described here. The angular dispersion of the nanograting was compensated for by adjusting the rotation and translation of the imaging gold mirror (see Fig. 3 for specific wavelengths). The entire setup is placed in a vacuum chamber and evacuated to a pressure of 10^{-5} mbar. Absorption of XUV light by residual gas in the chamber can thus be neglected. Our setup provided the possibility to measure the diffraction efficiency at any particular wavelength within the broad spectral range of the XUV source.

In order to independently calibrate the XUV intensity for each wavelength, we introduced a gold mirror into the beam instead of the nanograting as a reference. Both the grating and the XUV reflection mirror are situated on a translation stage. In order to avoid systematic drifts in the XUV spectrum from the HHG process (due to intensity fluctuations of the laser) to influence the measurement, alternating measurements were performed for the XUV intensity of the 0th diffraction order of the grating and the reflection from the mirror. In this way, the ratio $R_{0th/mirror}$ of the 0th diffraction order efficiency of the grating and the reflectivity of the mirror was determined (see black line in Fig. 4a). In order to measure the −1st order diffraction efficiency of the nanograting, the ratio $R_{-1st/0th}$ of the −1st and 0th order diffraction efficiencies was characterized. Note that $R_{-1st/0th}$ was corrected for the reflectivity of the second gold mirror for different incidence angles. The reflectivity of the gold mirror is derived from the refraction indices given in Palik's handbook [15].

#139920 - $15.00 USD Received 20 Dec 2010; revised 13 Jan 2011; accepted 13 Jan 2011; published 18 Jan 2011

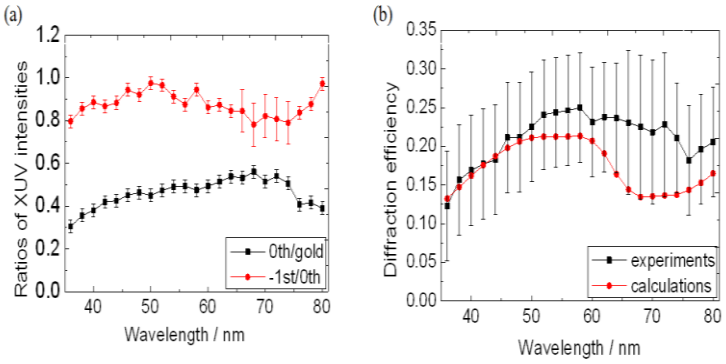

Fig. 4. (a) The measured ratios of XUV intensities. $R_{0th/gold}$ is the ratio of 0th order efficiency of the grating and gold mirror. The error bars given for the black curve stem from drifts in the XUV spectrum and are determined as 0.03. $R_{-1st/0th}$ is the ratio of −1st and 0th order efficiency of the grating. The error bars given for the red curve are statistical and correspond to the standard deviation (σ). (b) The calculated −1st order efficiency (red curve) and the extracted −1st order efficiency (black curve) from experiments. The error bars are based on the ones in (a) and they take into account systematic errors due to the calibration of the reflectivity by using the gold mirror. These errors are determined as 0.09 in the range from 66 nm to 74 nm and 0.07 at other wavelengths.

The output coupling efficiency of the −1st order, Eff_{-1st}, was extracted from the described measurements as follows:

$$\mathrm{Eff}_{-1\mathrm{st}}(\lambda) = \mathrm{R}_{-1\mathrm{st}/0\mathrm{th}}(\lambda) \times \mathrm{R}_{0\mathrm{th}/\mathrm{gold}}(\lambda) \times \mathrm{ref}_{\mathrm{gold}}(\lambda) \qquad (1)$$

where ref_{gold} is the gold reflectivity for different wavelengths. The result is displayed in Fig. 4b. In order to account for the limited resolution in the experimental measurements, the theoretical prediction that is displayed as red line in Fig. 4b has been convoluted with a Gaussian of 4 nm full-width at half-maximum. The experimental result is in reasonable agreement with the theoretical prediction. Notably, the experimental measurement around 70 nm gives a higher diffraction efficiency than theoretically predicted. At around 70 nm the refractive index of SiO_2 goes to 1, which leads to a dip in the −1st order diffraction. Although the dip is also evident in the measurement it is not as pronounced as in the theory. There are two potential reasons which could cause the deviations between the theoretical and experimental data. One is the roughness due to the fabrication limits of nanograting; the other is a possible change in the stoichiometric composition of the SiO_2 layer in the production process, which could affect the reflectivity of the dielectric surface of the grating in the XUV range.

To our best knowledge, this is the first full characterization of the −1st order XUV diffraction efficiency of a blazed nanograting. The fabricated dielectric nanograting exhibits a diffraction efficiency of more than 20% between 50 nm and 60 nm. Using such a blazed nanograting as output coupler in an enhancement cavity would result in high external XUV powers.

4. IR reflectivity and high-power nonlinearity of the blazed nanograting

In order to characterize the IR reflectivity of the nanograting, we used an optical lossmeter (LossPro, central wavelength 1030nm). Here, the mirror under test is implemented as one of the mirrors of a non-resonant cavity. A pulse is coupled to the cavity and the exponential decay of its intensity upon many bounces on the cavity mirrors is recorded. The total losses of the investigated mirror are calculated from a fit to the exponential decay, while the losses of the other cavity mirrors are known from a separate calibration measurement. To enable a continuous variation of the incidence angle on the investigated mirror, we have modified the

#139920 - $15.00 USD Received 20 Dec 2010; revised 13 Jan 2011; accepted 13 Jan 2011; published 18 Jan 2011

lossmeter cavity while keeping its length constant (which is crucial for an accurate measurement). We calibrated the modified cavity at the incidence angles for which the original device was designed, thus ensuring the reliability of our measurements. We compared the losses introduced by the nanograting to the losses of the original SiO_2 substrate of the dielectric mirror for different incidence angles (see Fig. 5). The reflectivity of the dielectric mirror is found to be larger than 99.994%. For the blazed grating, the IR reflectivity still remained large with more than 99.97%.

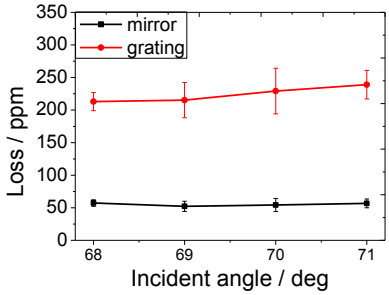

Fig. 5. The measured losses of the nanograting and dielectric mirror at the fundamental wavelength. The average of the loss of the grating is lower than 300 ppm (corresponding to a reflectivity > 99.97%), while the dielectric mirror without grating has a loss lower than 60 ppm (reflectivity > 99.994%). The error bars are statistical and correspond to the standard deviation (σ).

In order to investigate nonlinear effects at the nanograting, we used a z-scan setup shown in Fig. 6 and compared the properties of the nanograting with the dielectric mirror without grating.

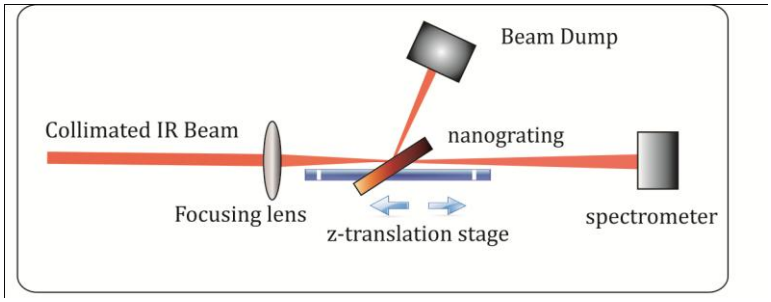

Fig. 6. Z-scan experimental setup: the nanograting is scanned under a 60° angle of incidence through the focused infrared laser beam with 1040 nm central wavelength, 40 W average power, 78 MHz repetition rate and 200 fs pulse duration. The signal transmitted through the mirror is monitored with an UV spectrometer. The focus of focusing lens is 150 mm, focus diameter is 55 µm, and collimated IR beam diameter is 3.6 mm.

We varied the intensity of an infrared laser beam impinging on the surface of the mirror with the nanograting structure by scanning it through a focus and monitored the third harmonic (TH) generated at the optical element and transmitted through it. The 3.6 mm diameter collimated output beam of the CPA system [17] is focused with a lens of an effective focal length of 150 mm down to 55 µm diameter. The laser parameters used here are: 1040 nm central wavelength, 40 W of average power, 78 MHz repetition rate and 200 fs pulse duration. A reproducible intensity variation is achieved by scanning the mirror along the optical axis (z-scan) through the focus. The angle of incidence on the mirror equals 60°, which is a geometrical constraint of our z-scan setup. The transmitted portion of the beam is sent to an UV spectrometer (Ocean Optics HR4000).

#139920 - $15.00 USD Received 20 Dec 2010; revised 13 Jan 2011; accepted 13 Jan 2011; published 18 Jan 2011

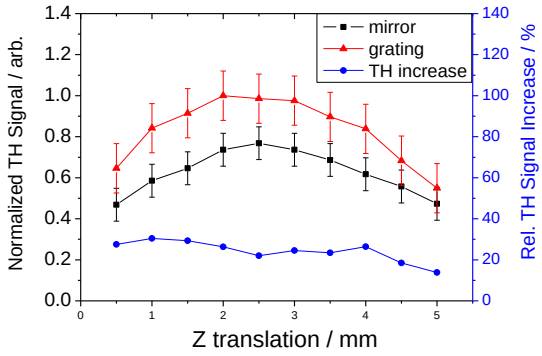

Fig. 7. Z-scan measurement results. The measurement gives insight into the optical properties of the high power nonlinearity introduced by the nanograting: the increase of the third harmonic intensities generated at the nanograting and at the plane surface of the same dielectric mirror is around 30%. The error bars for the red and black curves are statistical and correspond to the standard deviation (σ).

We investigated two cases: (i) the grating and (ii) a plane area on the same dielectric mirror surface was irradiated. For both cases we recorded the intensity of the TH (spectrometer counts at the third harmonic spectrum maximum), centered at 347 nm, as a function of the z position. The measurement for (i) has an absolute error of 0.12 in our measurement, and (ii) has an error of 0.08. Figure 7 shows the results. An enhancement of the TH is clearly visible in case of the nanograting. In comparison to the TH intensity generated at the dielectric mirror without grating, the TH intensity generated at the grating is increased by about 30%. Similar to the observed THG enhancement by the nanostructure on a dielectric substrate, THG enhancement was observed for metallic nanostructures attached to a dielectric, see e.g [18]. A detailed investigation of the physical mechanism behind this effect is the subject of future work.

This effect is likely to limit the maximum storable peak and / or average power as well as the minimum duration of the circulating pulse inside an enhancement cavity including the nanograting. On the one hand, with increasing intensities, THG introduces significant losses to the circulating field amplitude, affecting the enhancement. On the other hand, the THG, which is also observed from the plane mirror surface, might be correlated to an intensity-dependent variation of the nonlinear group velocity dispersion of the IR mirror. This effect has been observed in [19] for highly reflective mirrors. Despite these limitations, impressive values of 5 kW of circulating average power at a pulse duration of 120 fs and a repetition rate of 154 MHz were achieved in a cavity incorporating a nanograting recently [11]. Further scaling could be achieved with the approach of increasing the IR beam size on the nanograting, for instance using the cavity design presented in [20]. Moreover, not only the reflectivity of the optical element for the IR radiation, but also its diffraction efficiency in the XUV range could be altered in the high-power regime. These effects are subject to further investigation.

5. Conclusion

To conclude, we have designed, fabricated and characterized a blazed nanograting, which may serve as efficient output coupler for XUV radiation generated in a femtosecond enhancement cavity. A very high −1st order diffraction efficiency around 20% for the wavelength range from 35.5 nm to 79.2 nm was measured for the blazed nanograting. In addition to the XUV diffraction efficiency, we have measured the IR reflectivity and high-power non-linearities of such an optical element.

#139920 - $15.00 USD Received 20 Dec 2010; revised 13 Jan 2011; accepted 13 Jan 2011; published 18 Jan 2011

Acknowledgments

We acknowledge experimental support by Tino Eidam from the IAP, University of Jena. This work was supported by the BMBF under PhoNa - Photonische Nanomaterialien, contract number 03IS2101B, the DFG via the Emmy-Noether program and SPP1391. Y.-Y. Y. acknowledges support by a Chinese Academy of Sciences fellowship and S.L.S. acknowledges support by a fellowship of the Alexander von Humboldt foundation.

#139920 - $15.00 USD Received 20 Dec 2010; revised 13 Jan 2011; accepted 13 Jan 2011; published 18 Jan 2011